Power Electronic Conversion Technology Annex PECTA

European Conference on Power Electronics and Applications — Aalborg DENMARK — EPE'23 — September 4th > 8th, 2023 — ECCE EUROPE — www.epe2023.com

Switching losses in power devices: From dynamic on resistance to output capacitance hysteresis

Elison Matioli, Hongkeng Zhu, Nirmana Perera, Mohammad Samizadeh Nikoo, Armin Jafari, Remco van Erp
Ecole Polytechnique Federale de Lausanne (EPFL), Switzerland
E-Mail: elison.matioli@epfl.ch

Acknowledgments

This work has been conducted within PECTA, the Power Electronic Conversion Technology Annex. PECTA is part of the Technology Collaboration Programme 4E under the umbrella of the International Energy Agency.

Keywords

Conduction losses, switching losses, power semiconductor device, wide bandgap devices, Gallium Nitride (GaN)

Abstract

In this paper, we review some of the main methods to characterize on-state and off-state losses in wide-band-gap devices under switching conditions. In the off-state, we will discuss about losses related to charging and discharging the output capacitance in wide-band-gap devices, both in hard- and soft-switching. In the on-state, we will present an accurate measurement of dynamic on-resistance degradation, particularly in Gallium Nitride (GaN) devices. These losses are typically not described in data-sheets, but can be a dominant loss mechanism in power electronic applications.

I. Introduction

Wide-band-gap devices hold a huge promise for efficient power conversion due to their much lower on-state resistance as well as input and output charges, which enable them to switch at higher frequencies more efficiently than Si counterparts. Higher switching frequencies on the other hand, allow the reduction of energy storage components and thus, of the entire power converter, providing a significant increase in power density.

However, there are many factors that limit their potential to operate at higher frequencies. In the off-state, the charging and discharging process of output capacitance, in some cases, incur losses that scale with switching frequency. As a matter of fact, these losses can have important consequences both in soft- and hard-switching. In the on-state, it is well known that GaN devices present a larger on-resistance when switching, than their static value [1], [2]. In this paper, we will cover the different techniques to evaluate these losses, and show a comparison of them for different device technologies. Although such data is not present in data-sheets, here we show that for some applications, they can represent a significant portion of the entire device loss, affecting the design and efficiency of power converters.

II. Off-state losses: the role of output capacitance

A. Soft switching

In 2014, Fedisson et al. reported unexpected losses related to charging and discharging the output capacitance (C_o) of Si superjunction devices [3], which could not be explained with the

capacitance versus voltage (CV) curves from datasheets. This was later ascribed to the hysteresis in the device output capacitance [4]. Such losses are also reported in SiC [5], [6] and GaN devices [7], [8]. Different measurement techniques have been used to characterize the output capacitance hysteresis losses and are presented below:

a. Method 1: Sawyer-Tower

The Sawyer-Tower (ST) technique has traditionally been used for ferroelectric dielectric material characterization and recently has been adapted to characterize large-signal C_o of power devices [7], [9], [10]. The method relies on a simple topology based on only two voltage measurements. The device output charge characteristic (Q_o vs V_{ds}) is obtained by applying a large excitation voltage from a high-voltage amplifier to the DUT in off-state (with source and gate connected). A high-quality factor reference capacitor (C_{ref}) in series with the DUT is used to measure the DUT off-state charge, as the same current flows in both devices (Fig. 1). The energy loss dissipated during the cycle, E_{diss}, is then extracted by calculating the area between the charging and discharging QV curves. Measurement results for a planar Si device (Si-1) and a Si superjunction device (Si-4) from [9] are shown in Fig. 2.

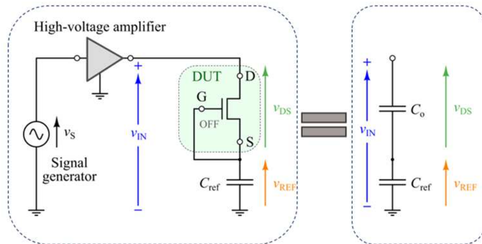

Fig. 1: Schematic of the power amplifier-based Sawyer-Tower measurement technique.

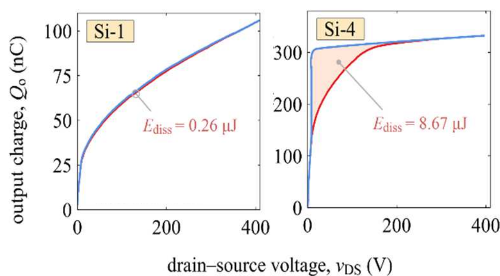

Fig. 2: Measurement results with ST technique for two different Si devices from [9].

Despite the simplicity of ST technique, a high-voltage power amplifier is required, whose bandwidth is usually limited to around 1 MHz, thus preventing measurements at higher frequencies. Also, the device is permanently in off state, excited by a continuous sinusoidal signal, which does not represent the real circuit operation.

b. Method 2: Nonlinear Resonance Method

Our group proposed a large signal measurement method for C_o hysteresis losses based on the nonlinear resonance (NR) between the device output capacitance and a high-quality-factor inductor (Fig. 3) [11]. The inductor, charged in the on-state, resonates with the device output capacitance, when the DUT is turned off, charging and discharging its C_o. The deviation between the measured drain-source voltage waveform during the charging and discharging processes corresponds to losses dissipated during the soft-switching transient, which can be calculated as

$$E_{diss} = \frac{1}{2L}(S_1^2 - S_2^2)$$

where S_1 and S_2 are the areas below the v_{ds} waveform during the charging and discharging process respectively [11].

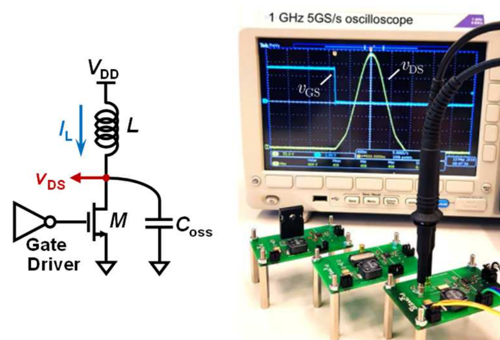

Fig. 3: Schematic of the nonlinear resonance (NR) measurement method and experimental setups.

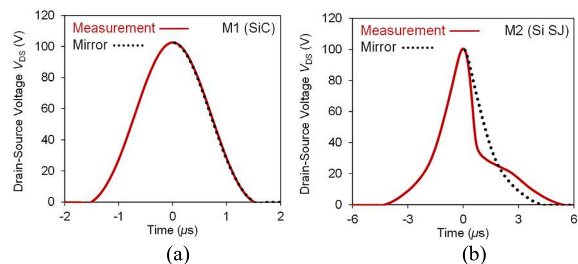

Fig. 4: Measured and mirrored v_{ds} waveforms for different power devices [11].

Fig. 4 shows the measured and mirrored v_{ds} waveforms for a SiC device and a Si superjunction (SJ) device. The measured resonant peak shows symmetrical charging/discharging process, thus lossless behavior for the SiC device (Fig. 4a). A nonsymmetrical process for the Si SJ is observed (Fig. 4b) [11], which corresponds to losses related to C_o charging/discharging.

The NR method is able to extract E_{diss} at high peak voltage (> 1000 V), high excitation frequency (> 40 MHz), and high dv/dt (> 120 V/ns). In addition, this method has a similar operation to actual resonant converters, which is not the case for the Sawyer tower method.

c. Method 3: Energy-based Nonlinear Resonance

Based on the nonlinear resonance between the device output capacitance and pre-calibrated inductor, we introduced an energy-oriented technique [12], in which the inductor current i_L is measured at the beginning and end of each pulse. E_{diss} is determined as the energy difference at the beginning ($E_0 = \frac{1}{2}LI_0^2$) and end ($E_1 = \frac{1}{2}LI_1^2$) of the resonance [12]. The energy loss in the inductor is equal to $2\pi/Q$, where Q is the inductor quality factor and must be as large as possible. Thus, the dissipated energy is

$$E_{diss} = (1 - \frac{2\pi}{Q})(E_0 - E_1)$$

This method considers the DUT as a black box regardless of the device model in the OFF-state and only requires current measurements after carefully characterizing the inductor.

Fig. 5 shows the measurement results using the energy-based technique for a Si SJ device, where only 7.7 uJ of the initial inductor energy (17.3 uJ) has been recovered after the charging and discharging process.

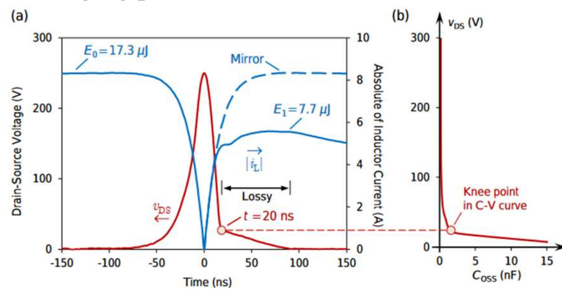

Fig. 5: Measured results for a Si SJ device [12].

d. Implications on a circuit level: Calorimetric Method

To emphasize the implication of C_o hysteresis losses on the circuit level, we proposed a calorimetric method [13] to measure the active device losses in a class-E inverter (Fig. 6). The choice of this circuit is the use of a single switch, which makes it easier to measure its losses. The heat generated by the active device during the converter operation is extracted by a silicon microfluidic channel-based cold plate with liquid cooling [14].

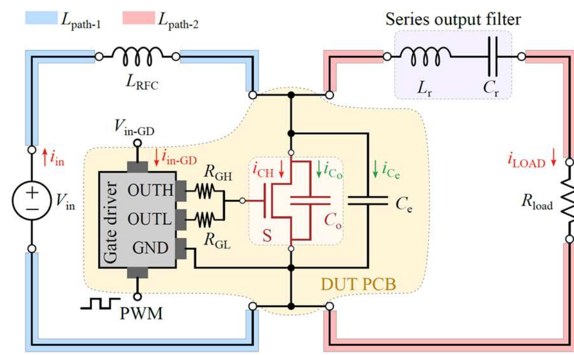

Fig. 6: Schematic of the class-E inverter.

The diagram of the measurement system and the experimental setup are shown in Fig. 7.

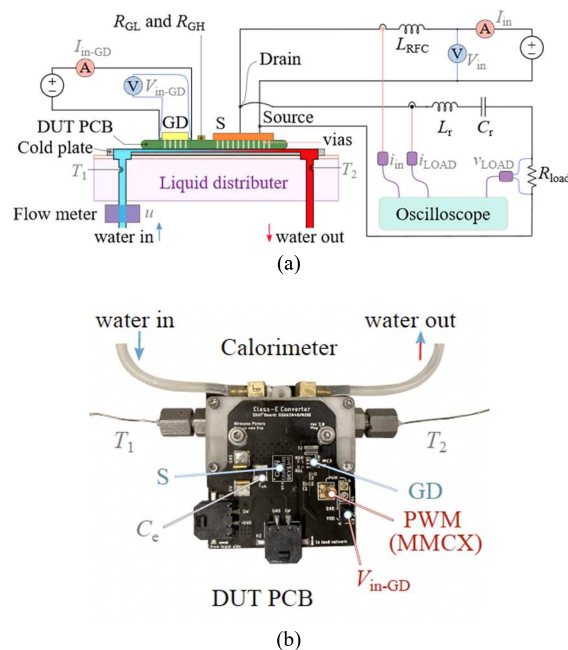

Fig. 7: (a) Simplified block diagram of the calorimetric measurement system and (b) hardware implementation.

The calorimetric system was verified with dc calibrations and can measure a wide power range from 20 mW to 10 W with an accuracy of 5%. This approach provides an accurate and in-converter evaluation of C_o hysteresis losses. By combining this calorimeter with electrical methods (to extract gate driving and conduction losses), a complete losses breakdown was obtained for a commercial GaN device (Fig. 8), which shows that the C_o hysteresis is the major loss contributor in MHz-range operations.

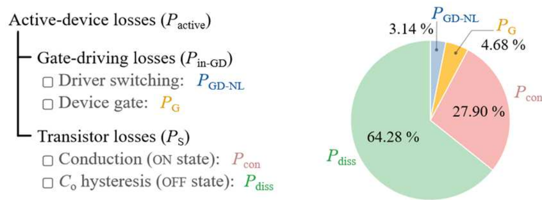

Fig. 8: Complete breakdown of the active device losses for a commercial GaN device at 10 MHz operation in the tested class-E inverter.

B. Hard switching

In hard-switching applications, the energy losses related to the output capacitance reflect the minimum switching energy and are load-independent. Conventional hard-switching tests cannot fully set apart the C_o-related hard-switching losses, and small-signal-based charge-voltage (QV) curves may fail to represent such large-signal losses.

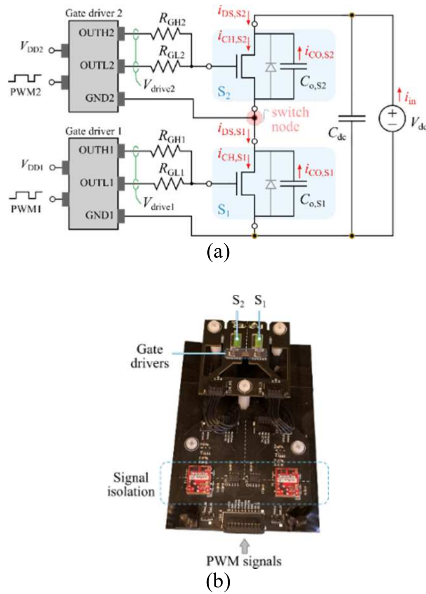

Fig. 9. (a) Schematic of the half-bridge no-load circuit where the devices are switched complementarily. (b) Experimental setup.

We developed a measurement technique to obtain the QV curves of power devices subjected to actual hard switching by using a half-bridge no-load circuit [15], as shown in Fig. 9.

The total turn-on energy related to C_o can be represented as

$$E_{on-Co} = Q_o V_{dc}$$

and the hard-switching QV curves can be obtained by sweeping V_{dc} and calculating the corresponding Q_o as

$$Q_o = \frac{1}{2}\frac{P_{in}}{V_{dc} f_{sw}}$$

where P_{in} is the average total input power measured with high-precision multimeters and f_{sw} is the switching frequency.

Experimental results for different types of power devices are shown in Fig. 10.

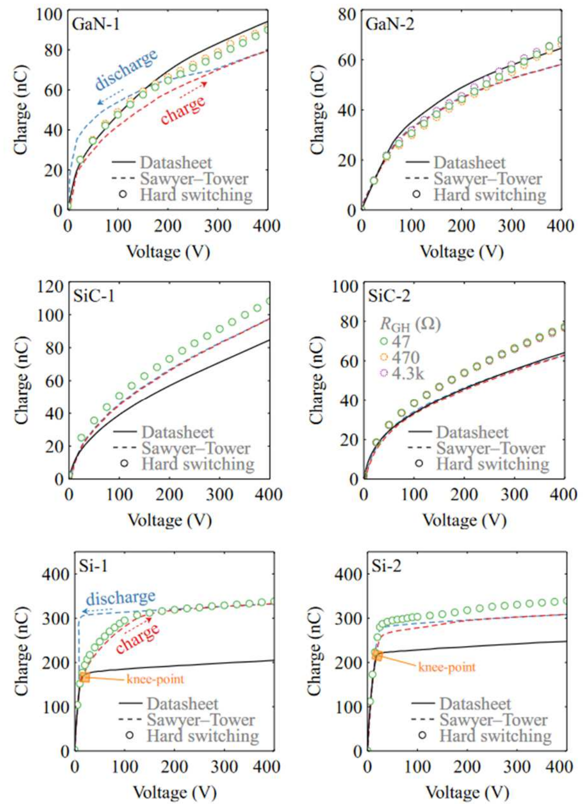

Fig. 10. Experimental QV curves obtained from the proposed hard-switching method for two GaN devices, two SiC devices, and two Si devices.

These results show that the large-signal behavior of Q_o in hard switching is highly dependent on device semiconductor technology. For certain devices, it cannot be predicted correctly based on data from datasheets or from soft-switching measurements. As concluded in ref. [15], datasheets could provide large-signal QV curves, and E_{on} should be separated into two parts to distinguish between the effects of C_o and load current.

III. ON-state losses: dynamic R_{ON} degradation

GaN devices often suffer from dynamic ON-resistance (R_{ON}) degradation, where R_{ON} increases right after the device turn-on due to electron trapping phenomena. Accurate measurement of dynamic R_{ON} is important to predict conduction losses for GaN HEMTs.

Most measurement methods for characterizing dynamic R_{ON} in the literature are based on pulsed measurements, whereas many conflicting results are reported even for the same device. In [16], we proposed a steady-state method to reveal true dynamic R_{ON} behaviors at real-circuit operations while decoupling the heating effects. The schematic and hardware circuit are shown in Fig. 11, which includes a hard-switching half-bridge and an active measurement circuit.

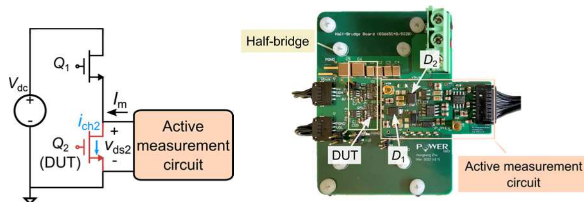

Fig. 11. Schematic and hardware circuit for the dynamic R_{ON} measurement at steady-state.

The active measurement circuit (Fig. 12) features OFF-state voltage blocking, diode voltage compensation, current sensing, and 50 Ω output impedance. It enables accurate and real-time measurements of dynamic R_{ON}, with a delay of less than 100 ns.

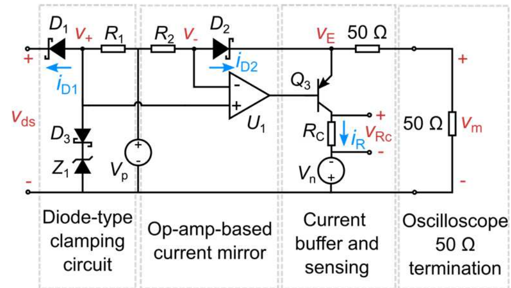

Fig. 12. Schematic of the active measurement circuit.

The dynamic R_{ON} behavior of a commercial Schottky-type p-GaN gate HEMT (GS66502B, 650 V/7.5 A) was investigated, and long transients up to 3 mins before R_{ON} stabilizes are observed, as shown in Fig. 13. Heating is not responsible for the transients before R_{ON} stabilizes as the temperature variance is small (< 4 °C) within the measurement window of 10 mins. Significant trapping and de-trapping time constants can be observed.

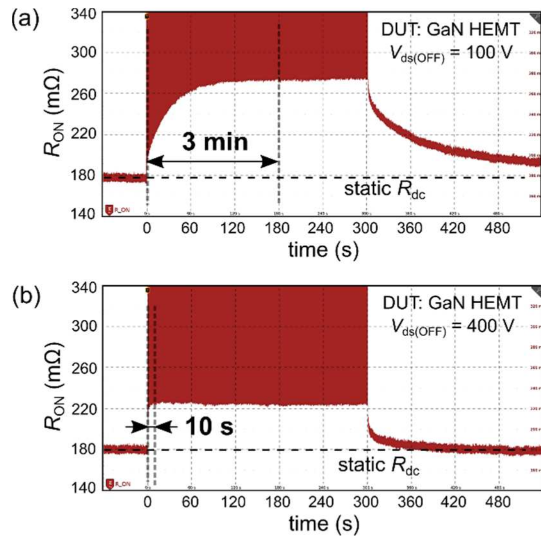

Fig. 13. Real-time monitoring of the dynamic R_{ON} before, during, and after switching at 10 kHz from t = 0 s for 5 mins at (a) $V_{ds(OFF)}$ = 100 V, and (b) $V_{ds(OFF)}$ = 400 V.

We also performed multi-pulse measurements to highlight the importance of steady-state methods. As shown in Fig. 14, multi-pulse tests with an arbitrary test time are not able to accurately capture the dynamic R_{ON} behavior at steady-state and may lead to wrong conclusions such that dynamic R_{ON} barely exists.

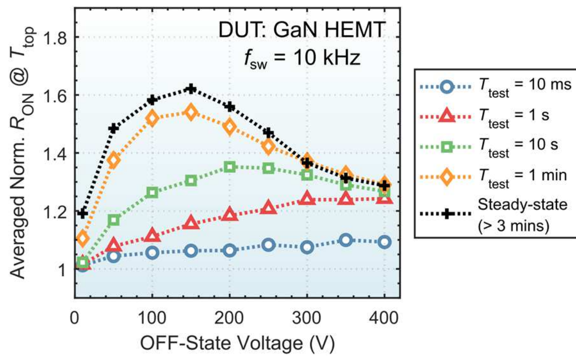

Fig. 14. Averaged normalized R_{ON} over the ON-time of the last pulse in multi-pulse tests at 10 kHz for a total test time ranging from 10 ms to 1 min.

With a consistent measurement method, we also evaluated dynamic R_{ON} at higher switching frequencies at steady-state and studied its effect, which can be used to predict the device conduction losses in real-circuit applications.

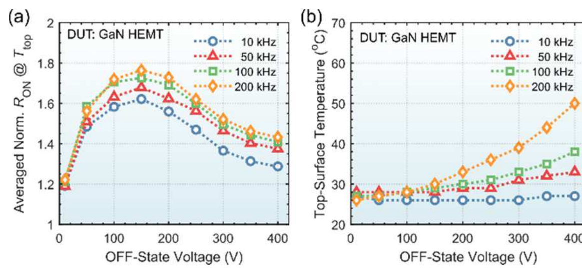

Fig. 15. (a) Averaged normalized R_{ON} of the GaN DUT over the ON-time at different switching frequencies and OFF-state voltages. (b) Top-surface temperature of the DUT measured under steady-state conditions.

As shown in Fig. 15, there is an increase in R_{ON} with frequency, which directly correlates to the long relaxation pattern during the ON-time. Furthermore, results are not influenced by temperature effects.

IV. Conclusion

This paper has discussed different methods for evaluating the OFF-state and ON-state losses for power semiconductor devices used in switched-mode power electronics. It is outlined that in soft-switching, the C_o hysteresis losses during the charging and discharging of C_o define an upper limit for switching frequency. In general, WBG devices offer much better soft-switching performance. In hard-switching, the actual output charge Q_o that determines the C_o-related hard-switching losses cannot be predicted from datasheet curves for certain devices. In terms of ON-state performance for GaN devices, we show that pulsed measurements with an arbitrary test time do not give an accurate picture of dynamic R_{ON} behavior. The proposed methods can be used to standardize measurements of losses in wide-bandgap devices, and benchmark different technologies.

References

[1] S. Yang, S. Han, K. Sheng, and K. J. Chen, 'Dynamic On-Resistance in GaN Power Devices: Mechanisms, Characterizations, and Modeling', IEEE Journal of Emerging and Selected Topics in Power Electronics, vol. 7, no. 3, pp. 1425–1439, Sep. 2019.

[2] G. Zulauf, M. Guacci, and J. W. Kolar, 'Dynamic on-Resistance in GaN-on-Si HEMTs: Origins, Dependencies, and Future Characterization Frameworks', IEEE Transactions on Power Electronics, vol. 35, no. 6, pp. 5581–5588, Jun. 2020.

[3] J. B. Fedison, M. Fornage, M. J. Harrison, and D. R. Zimmanck, 'Coss related energy loss in power MOSFETs used in zero-voltage-switched applications', in 2014 IEEE Applied Power Electronics Conference and Exposition - APEC 2014, Mar. 2014, pp. 150–156.

[4] J. B. Fedison and M. J. Harrison, 'Coss hysteresis in advanced superjunction MOSFETs', in 2016 IEEE Applied Power Electronics Conference and Exposition (APEC), Mar. 2016, pp. 247–252.

[5] G. Zulauf, Z. Tong, J. D. Plummer, and J. M. Rivas-Davila, 'Active Power Device Selection in High- and Very-High-Frequency Power Converters', IEEE Transactions on Power Electronics, vol. 34, no. 7, pp. 6818–6833, Jul. 2019.

[6] Z. Tong, J. Roig-Guitart, T. Neyer, J. D. Plummer, and J. M. Rivas-Davila, 'Origins of Soft-Switching C oss Losses in SiC Power MOSFETs and Diodes for Resonant Converter Applications', IEEE J. Emerg. Sel. Topics Power Electron., vol. 9, no. 4, pp. 4082–4095, Aug. 2021.

[7] G. Zulauf, S. Park, W. Liang, K. N. Surakitbovorn, and J. Rivas-Davila, 'COSS Losses in 600 V GaN Power Semiconductors in Soft-Switched, High- and Very-High-Frequency Power Converters', IEEE Transactions on Power Electronics, vol. 33, no. 12, pp. 10748–10763, Dec. 2018.

[8] M. Guacci et al., 'On the Origin of the $C_\textoss$ - Losses in Soft-Switching GaN-on-Si Power HEMTs', IEEE Journal of Emerging and Selected Topics in Power Electronics, vol. 7, no. 2, pp. 679–694, Jun. 2019.

[9] N. Perera, A. Jafari, L. Nela, G. Kampitsis, M. S. Nikoo, and E. Matioli, 'Output-Capacitance Hysteresis Losses of Field-Effect Transistors', in 2020 IEEE 21st Workshop on Control and Modeling for Power Electronics (COMPEL), Nov. 2020, pp. 1–8.

[10] N. Perera et al., 'Analysis of Large-Signal Output Capacitance of Transistors Using Sawyer–Tower Circuit', IEEE Journal of Emerging and Selected Topics in Power Electronics, vol. 9, no. 3, pp. 3647–3656, Jun. 2021.

[11] M. Samizadeh Nikoo, A. Jafari, N. Perera, and E. Matioli, 'Measurement of Large-Signal COSS and COSS Losses of Transistors Based on Nonlinear Resonance', IEEE

Transactions on Power Electronics, vol. 35, no. 3, pp. 2242–2246, Mar. 2020.

[12] M. S. Nikoo, A. Jafari, N. Perera, H. K. Yildirim, and E. Matioli, ‘Investigation on Output Capacitance Losses in Superjunction and GaN-on-Si Power Transistors’, in 2020 IEEE 9th International Power Electronics and Motion Control Conference (IPEMC2020-ECCE Asia), Nov. 2020, pp. 48–51.

[13] N. Perera, R. van Erp, J. Ançay, A. Jafari, and E. Matioli, ‘Active-Device Losses in Resonant Power Converters: A Case Study with Class-E Inverters’, in 2021 IEEE Energy Conversion Congress and Exposition (ECCE), Oct. 2021, pp. 5312–5319.

[14] R. van Erp, N. Perera, and E. Matioli, ‘Microchannel-based Calorimeter for Rapid and Accurate Loss Measurements on High-efficiency Power Converters’, in 2021 IEEE Energy Conversion Congress and Exposition (ECCE), Oct. 2021, pp. 5709–5715.

[15] N. Perera, A. Jafari, R. Soleimanzadeh, N. Bollier, S. G. Abeyratne and E. Matioli, "Hard-Switching Losses in Power FETs: The Role of Output Capacitance," in IEEE Transactions on Power Electronics, vol. 37, no. 7, pp. 7604-7616, July 2022.

[16] H. Zhu and E. Matioli, "Accurate Measurement of Dynamic ON-Resistance in GaN Transistors at Steady-State," in IEEE Transactions on Power Electronics, vol. 38, no. 7, pp. 8045-8050, July 2023